In search of nanoperfection: Experiment and Monte Carlo simulation of nucleation-controlled step doubling

Yi Wang, T. P. Pearl,[a] S. B. Darling, J. L. Gimmell, and S. J. Sibener[b]
James Franck Institute and Department of Chemistry, University of Chicago, 5640 South Ellis Avenue, Chicago, Illinois 60637

(Received 2 January 2002; accepted for publication 6 March 2002)

In order to make effective use of the extreme density of nanoscale elements that form spontaneously in self-assembling architectures, one must address the associated issue of minimizing defect creation during the formation of such structures. In this article we examine the competing roles that nucleation kinetics and two-dimensional growth processes play in nanostructure formation and defect minimization. We employ oxygen-induced step doubling of vicinal Ni(977) surfaces as our physical system, using elevated temperature scanning tunneling microscopy and Monte Carlo simulations to extract the desired details of interface evolution. Two interesting topological defect features are observed on the surface after doubling reaches its asymptotic limit: (i) ''frustrated ends,'' which form when two counter-propagating step-doubling events having a single step in common intersect, leaving a stable topological defect, and (ii) residual ''isolated single steps,'' which form when a single step is unable to partner with an adjacent step. This latter defect occurs when a single step is surrounded on both sides by previously doubled structures. In an attempt to understand and control these results, Monte Carlo simulations indicate that experimental control of the delicate and competing interplay of nucleation kinetics and two-dimensional growth kinetics is the key to the formation of more perfect interfaces. In this instance this corresponds to using a small initial oxygen exposure and reduced substrate temperature to achieve a doubled surface of higher perfection. Such optimized interfaces can act as templates for guiding the hierarchical assembly of nanowires and other nanoscale molecular assemblies.
[DOI: 10.1063/1.1473697]

I. INTRODUCTION

The atomic and nanoscale structure of surfaces, and the transformations between competing structures, depends upon the delicate balance of surface free energy terms which govern interfacial stability. Experiments that delineate the rich variety of interfacial structures which occur for both clean and adsorbate decorated surfaces have yielded a wealth of data on this issue, especially due to the advent of atomically resolved scanning probe microscopy. Vicinal (stepped) surfaces, in particular, have been observed to undergo a wide variety of surface reconstructions and structural phase transitions.[1–11] Time-lapse elevated temperature scanning tunneling microscopy measurements have recently allowed mechanistic details of such transitions to be delineated.[12,13] Images taken at latter times, when dynamical transformations have largely reached their asymptotic limit, reveal the existence of regions of relative structural perfection as well as regions that contain structural defects.

We have now come to appreciate that structural imperfections occur as a natural consequence of competing dynamical processes, such as nucleation kinetics and interface mobility. It is the purpose of this article to assess why such imperfections form, and to offer general routes to minimize their occurrence. This is important as the presence of structural imperfections certainly influences, and in many cases limits, the desirable chemical and physical properties of low-dimensional materials. For example, it is widely appreciated that the inherent properties of vicinal surfaces lend themselves to templating applications in which adsorbates, e.g., magnetic atoms, selectively decorate step edges, leading to fundamental systems for studying nanomagnetism and electronic transport in massively parallel arrays of nanowires.[14,15] Local imperfections limit the performance, and hence utility, of such templated nanostructures; to understand and experimentally control the extent of perfection of such interfaces is one of the key objectives on the road to implementing nanoscale textured interfaces for real-world applications.

Various experimental and theoretical studies have been performed to uncover the morphological evolution of stepped metal surfaces. Scattering techniques including low energy electron diffraction (LEED),[16] x-ray diffraction,[11] and helium atom scattering (HAS)[17] have been used to monitor structural phase transitions. In order to elucidate the local details of stepped surface behavior, time-lapse scanning tunneling microscopy (STM) has been employed on stepped metal surfaces.[12,13] There has been an increasing number of theoretical studies that seek to model the behavior of isolated steps on locally flat surfaces as well as stepped surfaces. Modeling efforts have been directed at issues that include step coalescence such as doubling,[18–20] facetting and step

[a]Present address: Dept. of Chemistry, Pennsylvania State University, University Park, PA 16802.
[b]Author to whom correspondence should be addressed; electronic mail: s-sibener@uchicago.edu

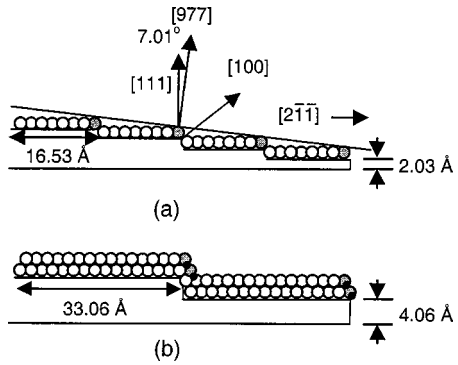

FIG. 1. A schematic of the (a) single step and (b) double step configurations for Ni(977). Several crystallographic dimensions and high symmetry directions are indicated. The clean, single step structure for this surface is composed of (111) terraces, eight atomic rows wide, separated by monatomic (100) risers. For the doubled surface, the (111) terraces extend to 15 atomic rows and the height is doubled. The oxygen that mediates the structural transition is adsorbed preferentially at the bottom of the steps.

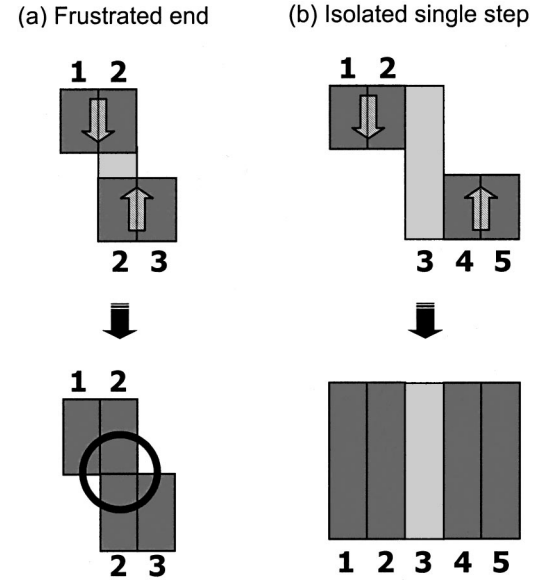

FIG. 2. Schematic illustrations of the processes leading to the formation of the two discussed surface defects: (a) frustrated ends and (b) isolated single steps. Both classes of defects prevent formation of a perfectly doubled surface. The darker and lighter shades represent double and single steps, respectively.

bunching,[21] step–step interaction energies,[22,23] roughening transitions,[24] and kink creation as a function of terrace width distribution.[20,24]

In the studies reported herein, we employ oxygen-induced step doubling of vicinal Ni(977) surfaces as our physical system, using elevated temperature scanning tunneling microscopy and Monte Carlo simulations to extract the desired details of interface evolution. Our results emphasize that the key control variables which govern step doubling and the ultimate quality of interface perfections are nucleation kinetics and two-dimensional mobility. While HAS experiments (and other reciprocal-space diffraction techniques) have provided useful data on the development of long-range order, it is the advent of local probes such as STM and atomic force microscopy which allows experimentalists to break the ensemble average and examine the formation and statistical properties of localized structures. We have designed and successfully constructed a variable-temperature ultrahigh vacuum (UHV) STM to enable such studies of local structure evolution, and related issues of local surface reactivity.[12,13,25]

II. EXPERIMENT

Experiments were performed in a stainless steel UHV chamber with a base pressure of 5.5×10^{-11} Torr equipped with an Omicron Micro STM adapted by us for elevated temperature imaging, and standard sample cleaning and characterization tools. Details of the design of the proximity heater and the UHV-STM system are given elsewhere.[25] The Ni(977) surface is a 7.01° miscut of a Ni(111) crystal in the [211] direction. In its unreconstructed step arrangement, this kinkless vicinal is composed of eight atomic row wide terraces of (111) symmetry separated by monatomic (100) step rises. The oxygen-driven reconstruction will double the surface steps both in width and height. Schematic illustrations of the Ni(977) surfaces with single and double steps are shown in Fig. 1. Experimental images were recorded between 400 and 470 K in constant current mode with a tunneling current of 1 nA and a 100 mV positive bias applied to the sample. Oxygen dosing was performed by chamber backfilling high purity O_2 using a high precision leak valve located in proximity to the STM. The listed oxygen exposures are the effective exposures to the surface region located directly beneath the STM tip, which are approximately 10% of the backfilling pressure. Sample preparation involved cycles of 1 keV Ar^+ sputtering between 300 and 1100 K and annealing by electron bombardment at 1100 K. Surface cleanliness was checked by Auger electron spectroscopy and crystallinity verified using LEED [sharp splitting of the (111) spots] and STM.

A STM experiment stars by locating a well-ordered region of single steps after a sputter and anneal cycle. After a favorable region is located, STM imaging is paused, oxygen is dosed by chamber backfilling, and imaging is resumed after the oxygen exposure is completed. Successive images are recorded until structural evolution reaches an asymptotic limit, which typically takes about 1 h.

III. RESULTS AND DISCUSSION

A. Experimental results

The oxygen-driven reconstruction dynamics and step merging mechanism of Ni(977) have been previously studied using both HAS[17] and STM.[12,13,26] It was found that steps commence coalescence at a point contact (i.e., a step-edge bulge connects to its downstairs neighbor step edge); and doubling then proceeds *via* bidirectional zippering. Under optimized oxygen coverage (step-edge saturation) at 465 K, the step doubling linear rate is ~3.7 Å s^{-1} corresponding to an areal sweep rate of ~60 Å^2 s^{-1} (the width of the propagating step terrace is ~16.5 Å).[13]

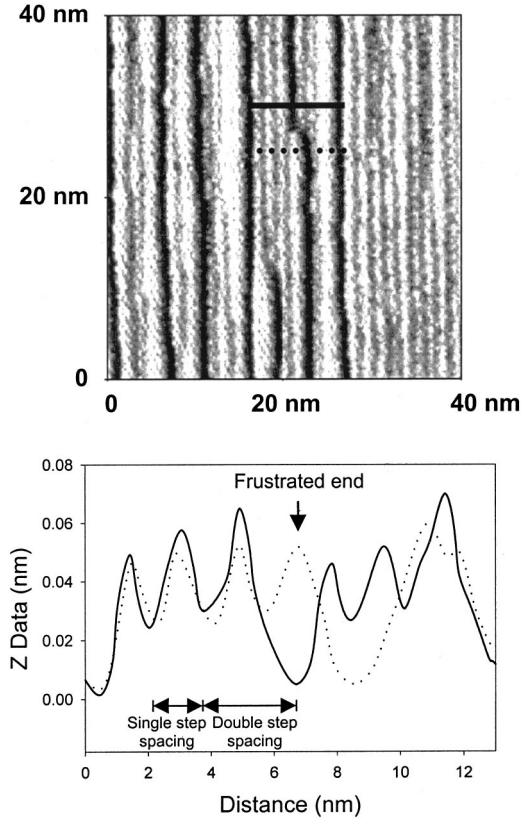

FIG. 3. Detailed structure of a frustrated end. Solid and dashed cuts of the image show the surface morphology on both sides of a frustrated end. The arrow in the lower panel marks the position of the frustrated end. The image shown is 40 nm×40 nm and was collected with 1 nA tunneling current and 100 mV sample bias.

With the dynamics and the mechanism of the reconstruction understood, we focused on several features that remained on the surface after the oxygen-driven step doubling reached its asymptotic limit. There are two possible defects that hinder perfect doubling: frustrated ''dead ends'' and isolated ''2-1-2'' single steps. Assume that there are initially three single steps: 1, 2, and 3. When the oxygen-induced doubling begins, steps 1 and 2 start to merge and begin growing from top to bottom. Meanwhile, steps 2 and 3 start to merge and begin growing from bottom to top. Their intersection forms a frustrated dead end. Experimentally, such frustrated ends are observed to remain stationary once formed, hence the reason why they are used as internal references to monitor surface morphology evolution.[12,13] For the isolated single steps, assume that initially there are five single steps: 1, 2, 3, 4, and 5. When steps 1-2 and 4-5 are doubled, 3 remains as an isolated single step having no neighbor with which it can merge.

Figure 2 contains schematic pictures of the frustrated end and isolated single step anomalies. These two features are important since, ideally, they are the only possible defects that can inhibit the formation of a perfectly doubled surface. Studying the relationship between their formation and the experimental conditions helps further our understanding of step doubling and facetting phenomena, enabling the production of more perfect surface patterns for use as nanoscale templates.

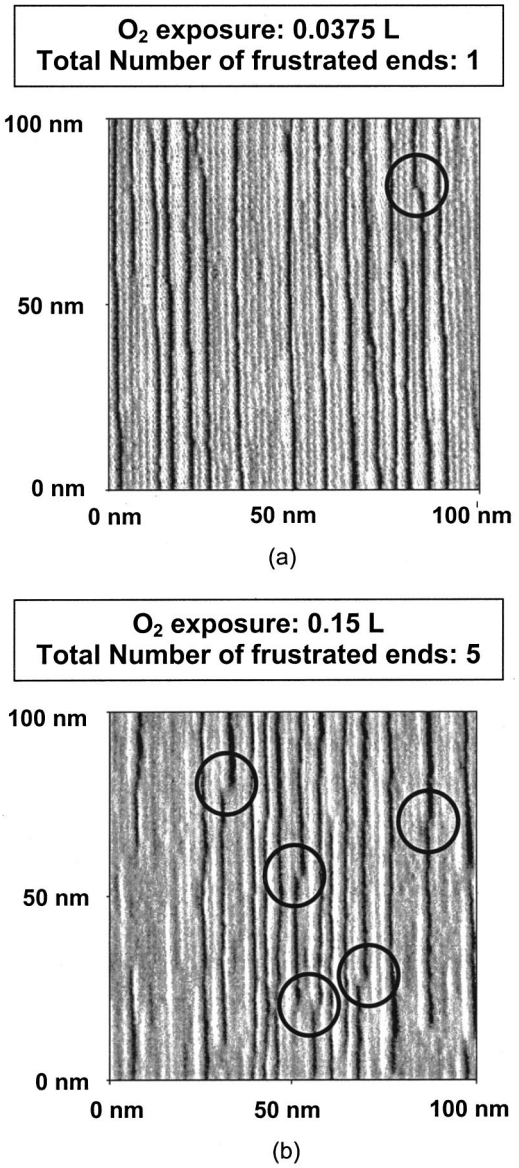

FIG. 4. Experimental results demonstrating the relation between initial oxygen exposure and the total number of frustrated ends with: (a) 0.0375 L O_2 exposure and (b) 0.15 L O_2 exposure. The image shown is 100 nm×100 nm and was collected with 1 nA tunneling current and 100 mV sample bias at 465 K. The surface depicted in (a) contained some inherent double steps before exposure to oxygen.

Figure 3 is an image of an isolated frustrated end. The solid and dashed lines show the height profile of the metal surface on the top and bottom of the frustrated end, respectively. Figure 4 contains two final-stage images that resulted from two different initial oxygen exposures. The frustrated ends are marked with circles. Small oxygen exposure (0.0375 L) results in only one frustrated end, while larger oxygen exposure (0.15 L) leads to five frustrated ends. The ultimate number of frustrated ends depends on both the nucleation rate (the rate for generating the initial contact points) and the step zippering rate. The relationship between the initial oxygen exposure and the total number of frustrated ends, analyzed over a 100 nm×100 nm area for multiple doubling experiments, is summarized in Fig. 5. It is clear that the initial oxygen exposure is proportional to the ultimate

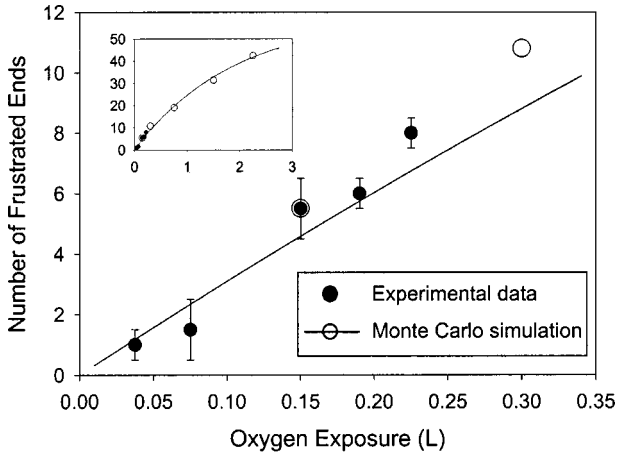

FIG. 5. Relationship between initial oxygen exposure and the total number of frustrated ends on a 100 nm×100 nm area. The solid circles are experimental data while the open circles are the Monte Carlo prediction. The simulation data are normalized to the experimental data at a single point (optimal oxygen exposure). The solid line is an exponential fit to the simulation results and the inset shows a larger range of parameter values. Note that the fit is applied to the entire range of simulation data as shown in the inset.

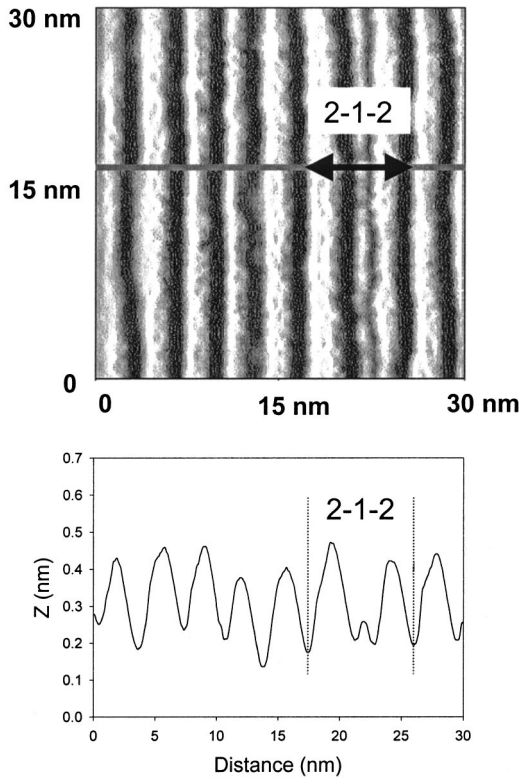

FIG. 6. Detailed structure of an isolated single step. In the height profile illustrated in the lower panel, there is one instance visible.

number of frustrated ends. Even before the oxygen exposure reaches its optimal value (0.15 L), additional oxygen increases the probability of forming contact points between two neighboring steps, and therefore increases the probability of forming frustrated ends. When the oxygen exposure is beyond the optimal value, the nucleation rate remains virtually unchanged, but the extra adsorbed oxygen hinders step zippering.[12,13] In effect, this too increases the probability of forming frustrated ends. The effect of the nucleation and zippering rates on the ultimate number of frustrated ends will be discussed later.

In addition to dead ends, isolated single steps also remain on the surface. A characteristic structure is presented in Fig. 6. The ultimate isolated single step populations for experimental images (100 nm×100 nm) range from 11% to 17% with an average of 15% and do not show an obvious dependence on the initial oxygen exposure. Under ideal conditions (i.e., no frustrated ends), the best result will be a perfectly doubled surface with 0% isolated single steps and the worst result will be 20% isolated single steps. A simple statistical model using various $(1\times N)$ matrices, with N ranging from 10^1 to 10^5, was used to determine the expected single step population excluding the effect of frustrated ends. Statistically, one expects approximately 13.5% isolated single steps, agreeing well with the observed population.

B. Monte Carlo simulation

Monte Carlo simulation of this phenomenon was performed using a simple physical model based on extant experimental understanding for oxygen-driven Ni(977) step doubling.[12,13,17] The doubling process is enabled by the formation of an initial point contact between a meandering upper step edge, pinned by oxygen atoms adsorbed on the (100) step face.[18] Our simulation study focuses on the final state of the surface, in particular defect content, in order to understand the relationship between experimental conditions and surface structure upon reaching an asymptotic limit.

An $(N\times N+1)$ matrix was used to mimic the Ni(977) surface, where N is a positive integer. Every column of the matrix is regarded as a single surface step. Two experimental conditions were set as parameters: nucleation rate (the rate for generating the initial contact points) and step zippering rate after the first point contact was made. Since the nucleation rate and the zippering rate are both related to the local oxygen coverage at the step edges and the temperature, it is possible to connect the simulation results to the experimental findings to further our understanding and guide future experiments.

After a certain size matrix is chosen, several simulation rules are constructed:

(1) The positions of the initial nuclei (contact points) are chosen randomly in the matrix.

(2) A nucleus can only combine with its right-side (downstairs) neighbor, if available, to initiate doubling. This restriction is introduced because, as seen in our experimental studies of Ni(977) doubling, initial contact between neighboring single steps occurs only in the downstairs direction.[12,13,26]

(3) After every cycle of the program, a fixed number of nuclei will be chosen randomly only from the *unoccupied* positions in the matrix. In this context, ''unoccupied'' means the site has not been chosen as a nucleus nor been doubled via zippering before this cycle. This is because, in the comparative experiment, the step edges were fully decorated with oxygen before step doubling, enabling every step-edge site

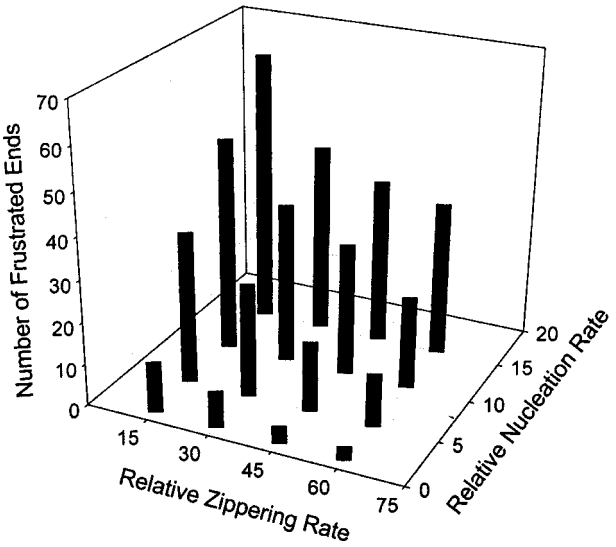

FIG. 7. Monte Carlo simulation results for the relationship between the nucleation rate, zippering rate, and the total number of frustrated ends. Lower zippering rate or higher nucleation rate lead to more frustrated ends.

on the surface to serve as a nucleus. Unlike experiments such as adsorption–decomposition of gas-phase compounds on surfaces, whose nucleation rate is limited by the dose rate, the preadsorbed oxygen on the Ni(977) surface prepares every step site for possible merging with its downstairs neighbor. For a fixed period of time, a fixed number of nuclei will appear on the surface with those nuclei initiating zippering in both directions during the next cycle and thereafter. Zippering occurs at a preselected rate (zippering rate). Details of this experimentally observed zippering process have been described previously.[13]

(4) The simulation will stop when creation of a new nucleus is impossible, i.e., the surface is composed only of doubled steps, frustrated ends, and isolated single steps.

(5) The final results of the simulation are averaged over many completed runs.

To compare directly with 100 nm×100 nm experimental images, a (60×61) matrix was used for the simulation since the Ni(977) single step width is 1.65 nm; with these dimensions each matrix column represents one singled terrace. Moreover, boundary conditions are another important consideration. Monte Carlo simulations were actually executed for a larger matrix, and only the central (60×61) region was analyzed. We varied the matrix size through a considerable range and found that, for matrices larger than (100×101), the calculation results remain unchanged. For the following results, a (120×121) matrix was chosen to study the effect of the nucleation and zippering rates on the final surface morphology. The extra column is introduced in order for every step to have a right-side neighbor.

Figure 7 plots the total number of frustrated ends as a function of the nucleation and zippering rates. The simulation results exhibit a clear effect: the higher the nucleation rate, the more dead ends; the higher the zippering rate, the fewer dead ends; and if the ratio of the nucleation rate and the zippering rate is kept constant, the larger their absolute magnitudes, the more frustrated ends. Also, the ultimate number of frustrated ends is not as sensitive to the zippering rate as it is to the nucleation rate. The relation between the nucleation rate or the zippering rate and the total number of frustrated ends is as expected. The nucleation rate increases as the step mobility increases, that is, the higher the possibility for two steps to stick together and to possibly form a frustrated end. A faster zippering rate will allow the step doubling to be completed in a shorter time, thereby minimizing the number of nucleation sites and decreasing the ultimate number of frustrated ends. However, the result that the total number of frustrated ends depends on the absolute magnitudes of these two rates (with their ratio constant) is somewhat unintuitive. This scaling behavior is a consequence of the time step of the simulation because more than one nucleation event can occur in a given calculation cycle. Simulation results for the final percentage of isolated steps fluctuate between 13.0% and 14.5% and do not show a strong dependence on either nucleation or zippering rate. This result agrees well with the population predicted by the one-dimensional statistical model described above. An analytical solution of $1/e^2$ (0.135) for a different physical system with a similar mathematical description to our one-dimensional model was reported in 1939 by Flory.[27]

C. Comparison between experiments and Monte Carlo simulation

By comparing experimental data with Monte Carlo simulation results, a physical calibration can be applied to the simulation parameters. With this correspondence in hand, it will be possible to design future experiments that incorporate optimized substrate conditions. It is known that when the initial oxygen exposure is 0.15 L, the step zippering rate is 3.7 Å s^{-1} at 465 K.[13] When the step doubling reaches an asymptotic limit, the total number of frustrated ends is 5–6 on a 100 nm × 100 nm surface sample, and the final percentage of isolated single steps is ~15%.

Since the final percentage of isolated single steps is not sensitive to either the nucleation or the zippering rate, we use the total number of frustrated ends as the comparison criterion. To achieve 5–6 frustrated ends on a 100 nm×100 nm area, the corresponding simulation parameters for a 60×61 matrix are a nucleation rate of 1 and a zippering rate of 43. Assuming each element of the matrix is a square, the length of each element will be 16.5 Å, which is equal to the Ni(977) terrace width. Therefore, in every program cycle, the zippering distance will be 100 nm×(43/60)=71.7 nm. Since the experimental zippering rate is 3.7 Å s^{-1} at 465 K, one assigns every program cycle to 71.7 nm/0.37 nm s^{-1}=194 s at this temperature. Hence, on a 100 nm×100 nm Ni(977) surface, we would expect to see about 3600 s/194 s≈19 nucleation sites (point contacts) within 1 h under these conditions. Given the timescales of imaging, it is unfeasible to catch the formation of every individual nucleus. If multiple nuclei form on a certain step, the exact number of them often cannot be determined by examining discrete STM images. The simulation, therefore, enhances our understanding of this phenomenon by providing insight into the true nucleation rate.

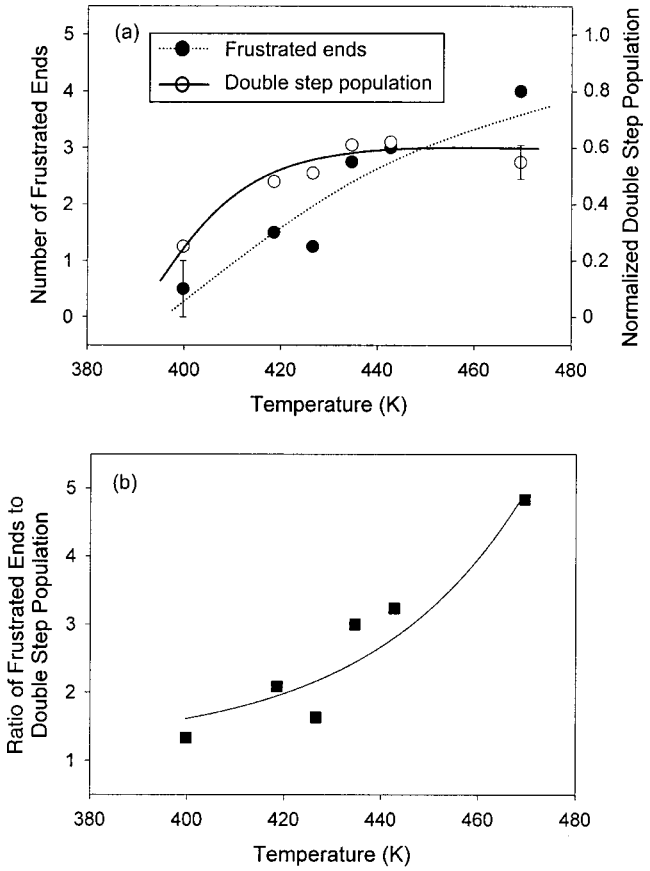

FIG. 8. (a) Temperature dependence of frustrated end generation and doubling extracted from STM data. The filled circles show the number of frustrated end defects in a 100 nm×100 nm area, the open circles show the percent conversion to double steps. Representative error bars are included for one point in each data set. Lines through the data show the qualitative trends. (b) The ratio of frustrated ends to double step population with the fitted line serving as a guide to the observed trend. This ratio increases monotonically with temperature; at higher temperatures there is little net gain in conversion, yet many more defects are nucleated.

By analyzing the Monte Carlo simulation, the effects of both the nucleation rate and the zippering rate on step doubling are better understood. If the goal is to make a perfectly doubled Ni(977) surface, the key factor is to minimize the total number of frustrated ends while enabling the most doubling to occur. In order to prevent the formation of these defects, a low nucleation rate and a high zippering rate are required. For a doubling event to occur, the steps need to be mobile enough to have a significant probability of overcoming entropic repulsions. Nucleation and subsequent zippering then occur provided that both steps are decorated with oxygen. In order to minimize the number of frustrated ends, the nucleation events need to be controlled. By using a small initial oxygen exposure, the nucleation rate could be reduced. However, this will result in incomplete step doubling since the total amount of oxygen would not be enough to cover all the step edges. Mastering this balance is key to generating a more perfectly doubled surface.

Since the simulation results show that the final number of frustrated ends is not as sensitive to the zippering rate as it is to the nucleation rate, lowering the temperature will likely be effective in enhancing the extent of perfection of the asymptotic surface. The steps will zipper slightly slower than at the upper end of the temperature regime, but the nucleation rate will be affected far more dramatically, thereby minimizing the number of frustrated ends. Preliminary experiments testing this hypothesis drawn from our simulations have confirmed this methodology. Figure 8 depicts data extracted from a series of STM scans performed at different temperatures. Final state images (100 nm×100 nm) of doubling sequences recorded between 400 and 470 K for 0.15 L oxygen were analyzed to assess the effect of temperature on frustrated end creation compared to the extent of doubling. While the general trend is increasing for both the desired conversion to double steps and the number of unwanted frustrated end defects with higher temperature, the ratio between these two values is not linear. One can gain conversion with only mild increases in defects up to a temperature of approximately 425 K. At higher temperatures, there is little further net conversion, yet many more defects are introduced.

In summary, the conditions for producing more perfectly doubled steps lie more in tuning the temperature than the oxygen exposure. Future experiments on this system will determine how effective these adjustments are in minimizing defect formation. Further Monte Carlo simulations will focus on nanowire formation *via* gas decomposition and deposition on solid vicinal surfaces. Moreover, subtle but potentially quite important correlations involving the dynamics of neighboring steps (see Fig. 9 in Ref. 13) can be introduced into the simulation. Taking advantage of such interstep communication may be necessary to achieve more perfect conversion.

IV. CONCLUSIONS

In this article we have critically examined, combining experiment and numerical simulation, the key control parameters that govern the formation of relatively defect-free modified-structure vicinal surfaces. We have employed oxygen-induced step doubling of Ni(977) surfaces as our physical system using elevated temperatures STM and Monte Carlo simulations to extract the desired details of interface evolution. These studies have elucidated the competing roles that nucleation kinetics and two-dimensional growth processes play in nanostructure formation and defect minimization. Elevated temperature STM has been used to probe the oxygen-induced reconstruction behavior of Ni(977). Special attention was paid to characterizing the morphological features that remained on the surface after the step doubling process reached its asymptotic limit.

Two interesting topological defect features were the primary focus: frustrated ends, which occur when two doubling events growing from opposite directions and sharing a common single step meet each other, and isolated single steps, which are single steps surrounded by double steps rendering them unable to reconstruct. Correlations between a wide range of experimental parameters and asymptotic surface structure were elaborated. These insights were further elaborated using Monte Carlo simulations. The final number of frustrated ends was shown to increase with increasing nucle-

ation rate, and to decrease with increased zippering rate. There is no dependence of the final isolated single step coverage on either rate. STM studies have also demonstrated that one can gain conversion to double steps with only mild increases in the density of frustrated ends up to ~425 K. Further temperature increases produce little further conversion and a higher level of defects.

Studies involving the growth of nanoscale wires using stepped surfaces as a template are now in progress in our group. Recently, semiconductor nanowires have been demonstrated to operate as $p-n$ junctions, transistors, and complimentary inverters.[28–30] Synthesis of these wires has progressed in the last few years, but alignment of multiple wires is still a problem. Such findings, coupled with the production of variable-dimension stepped-surface guides, imply that semiconductor nanowires templated on vicinal surfaces have the potential to serve as building blocks for massively parallel nanoelectronic and magnetic devices. Moreover, one can speculate that a similar self-alignment approach can be employed for the construction of nanofluidic channel assemblies. This procedure would involve first decorating step edges with one compound followed by deposition of a multilayer matrix; the step edge compound could then be dissolved or etched away leaving aligned nanoscale channels for fluid transport. The work herein reported represents a clear step to realizing the technological utilization of such nanoscale constructs.

ACKNOWLEDGMENTS

The authors would like to thank Thomas Witten and Ajay Gopinathan for bringing Ref. 27 to our attention and Aaron Rosenbaum for useful discussions. Special appreciation is due to John Light and Kevin Gibson for their help in developing the simulation program. This work was supported by the Chemical Sciences, Geosciences and Biosciences Division, Office of Basic Energy Sciences, Office of Science, U.S. Department of Energy, Grant No. DE-FG02-00ER15089. Jennifer Gimmel acknowledges summer scholarship support from the University of Chicago Materials Center through its Research Experience for Undergraduates program.

[1] G. Comsa, G. Mechterscheimer, and B. Poelsema, Surf. Sci. **119**, 159 (1982).
[2] E. Hahn, A. Fricke, H. Röder, and K. Kern, Surf. Sci. **297**, 19 (1993).
[3] E. Hahn, H. Schief, V. Marsico, A. Fricke, and K. Kern, Phys. Rev. Lett. **72**, 3378 (1994).
[4] B. Lang, R. W. Joyner, and G. A. Somorjai, Surf. Sci. **30**, 454 (1972).
[5] J. E. Ortega, S. Speller, A. R. Bachmann, A. Mascaraque, E. G. Michel, A. Närmann, A. Mugarza, A. Rubio, and F. J. Himpsel, Phys. Rev. Lett. **84**, 6110 (2000).
[6] J. P. Chang and J. M. Blakely, J. Vac. Sci. Technol. A **10**, 2154 (1992).
[7] O. Haase, R. Koch, M. Borbonus, and K. H. Rieder, Phys. Rev. Lett. **66**, 1725 (1991).
[8] R. Koch, O. Haase, M. Borbonus, and K. H. Rieder, Surf. Sci. **272**, 17 (1992).
[9] H. E. Dorsett, E. P. Go, J. E. Reutt-Robey, and N. C. Bartelt, Surf. Sci. **342**, 261 (1995).
[10] D. G. Castner and G. A. Somorjai, Surf. Sci. **83**, 60 (1979).
[11] G. M. Watson, D. Gibbs, S. Song, A. R. Sandy, S. G. Mochrie, and D. M. Zehner, Phys. Rev. B **52**, 12329 (1995).
[12] T. P. Pearl and S. J. Sibener, J. Chem. Phys. **115**, 1916 (2001).
[13] T. P. Pearl and S. J. Sibener, J. Phys. Chem. B **105**, 6300 (2001).
[14] D. Li, B. R. Cuenya, J. Pearson, S. D. Bader, and W. Keune, Phys. Rev. B **64**, 144410/1 (2001).
[15] F. J. Himpsel, T. Jung, and J. E. Ortega, Surf. Rev. Lett. **4**, 371 (1999).
[16] T. P. Pearl, S. B. Darling, and S. J. Sibener, Surf. Sci. **491**, 140 (2001).
[17] L. Niu, D. D. Koleske, D. J. Gasper, S. F. King, and S. J. Sibener, Surf. Sci. **356**, 144 (1996).
[18] T. L. Einstein, T. M. Jung, N. C. Bartelt, and E. D. Williams, J. Vac. Sci. Technol. A **10**, 2600 (1992).
[19] T. M. Jung, R. J. Phaneuf, and E. D. Williams, Surf. Sci. **254**, 235 (1991).
[20] S. V. Khare, T. L. Einstein, and N. C. Bartelt, Surf. Sci. **339**, 353 (1995).
[21] M. I. Larsson, Phys. Rev. B **56**, 15157 (1997).
[22] E. L. Goff, L. Barbier, L. Masson, and B. Salanon, Surf. Sci. **432**, 139 (1999).
[23] H. C. Jeong and J. D. Weeks, Surf. Sci. **432**, 101 (1999).
[24] L. Barbier, L. Masson, J. Cousty, and B. Salanon, Surf. Sci. **345**, 197 (1996).
[25] T. P. Pearl and S. J. Sibener, Rev. Sci. Instrum. **71**, 124 (2000).
[26] T. P. Pearl and S. J. Sibener, Surf. Sci. Lett. **496**, L29 (2002).
[27] P. J. Flory, J. Am. Chem. Soc. **61**, 1518 (1939).
[28] Y. Cui, X. Duan, J. Hu, and C. M. Lieber, J. Phys. Chem. B **104**, 5213 (2000).
[29] S. W. Chung, J. Y. Yu, and J. R. Heath, Appl. Phys. Lett. **76**, 2068 (2000).
[30] Y. Cui and C. M. Lieber, Science **291**, 851 (2001).